

MAGNETOSPHERIC MULTISCALE MISSION (MMS) PHASE 2B NAVIGATION PERFORMANCE

Paige Thomas Scaperoth,^{*} Anne Long[†] and, Russell Carpenter[‡]

The Magnetospheric Multiscale (MMS) formation flying mission, which consists of four spacecraft flying in a tetrahedral formation, has challenging navigation requirements associated with determining and maintaining the relative separations required to meet the science requirements. The baseline navigation concept for MMS is for each spacecraft to independently estimate its position, velocity and clock states using GPS pseudorange data provided by the Goddard Space Flight Center-developed Navigator receiver and maneuver acceleration measurements provided by the spacecraft's attitude control subsystem. State estimation is performed onboard in real-time using the Goddard Enhanced Onboard Navigation System flight software, which is embedded in the Navigator receiver. The current concept of operations for formation maintenance consists of a sequence of two maintenance maneuvers that is performed every 2 weeks. Phase 2b of the MMS mission, in which the spacecraft are in 1.2×25 Earth radii orbits with nominal separations at apogee ranging from 30 km to 400 km, has the most challenging navigation requirements because, during this phase, GPS signal acquisition is restricted to less than one day of the 2.8-day orbit. This paper summarizes the results from high-fidelity simulations to determine if the MMS navigation requirements can be met between and immediately following the maintenance maneuver sequence in Phase 2b.

INTRODUCTION

The Magnetospheric Multiscale (MMS) mission will investigate the reconnection of charged particles in Earth's magnetosphere through the use of four spacecraft flying in a tetrahedral formation. To meet the science requirements for this mission, the spacecraft must maintain minimum relative separations which result in challenging navigation requirements. The current plan to sustain these minimum separations is to perform formation maintenance maneuvers every 2 weeks. Each sequence consists of two maneuvers; the first takes place at a True Anomaly of 202° and the second at a True Anomaly of 158° . This mission comprises two science phases. In Phase 1 the spacecraft are in 1.2×12 Earth radii orbits with nominal separations at apogee ranging from 10 km to 160 km. In Phase 2b, the spacecraft are in 1.2×25 Earth radii orbits with nominal separations at apogee ranging from 30 km to 400 km. Phase 2b has the most challenging navigation requirements because GPS signal acquisition is not permitted in the science region of interest (ROI), resulting in less than one day of GPS tracking during the 2.8-day orbit. Figure 1 illustrates the reference orbital geometry during MMS Phase 2b.

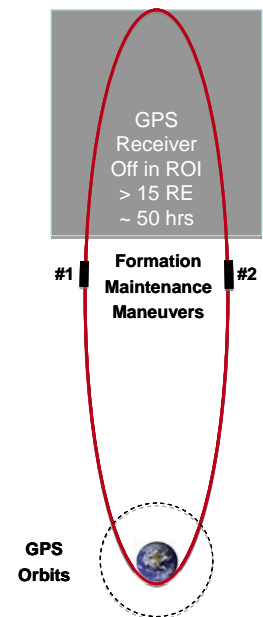


Figure 1: MMS
Phase 2b Geometry

^{*} Aerospace Engineer, a.i. solutions, Inc., 10001 Derekwood Lane; Lanham, MD 20706.

[†] Chief Systems Engineer, a.i. solutions, Inc., 10001 Derekwood Lane; Lanham, MD 20706

[‡] Aerospace Engineer, Code 595 NASA Goddard Space Flight Center; Greenbelt, Maryland 20771.

The current navigation concept for the MMS mission is for each spacecraft to independently estimate its position, velocity and clock states using GPS pseudorange data. The Goddard Space Flight Center (GSFC)-developed Navigator receiver will provide the GPS pseudorange data and maneuver acceleration measurements will be provided by the spacecraft's attitude control subsystem. The Goddard Enhanced Onboard Navigation System (GEONS) flight software, which is embedded in the Navigator receiver, will be used to perform state estimation onboard in real-time.

The focus of this paper is verification that the MMS navigation requirements can be met during Phase 2b. This paper presents results from a closed loop orbit control simulation for a Phase 2b formation with a mean separation of 25km during the Region Of Interest (ROI) and minimum separation of 8 km.[§] In this simulation, the effects of navigation errors on the planned maneuvers and maneuver acceleration errors on the navigation estimates are accurately modeled. In all simulations, Navigator performance characteristics are consistent with measured performance. Navigation performance is evaluated with respect to the following navigation requirements:

1. Definitive Absolute Orbit Determination - During the science phases of the mission, the definitive RSS absolute position error of each spacecraft in the MMS constellation shall not exceed 100km, with 99% probability.
2. Definitive Relative Orbit Determination - During the science ROI, the definitive RSS relative position error between each pair of spacecraft in the MMS constellation shall not exceed the greater of 1 percent of their scalar separation or 100m, with 99% probability.
3. Predictive Relative Orbit Determination - During all phases except commissioning and maneuver recovery, the relative position error RSS growth rate of the premaneuver 7-day predictive orbit determination solution shall not exceed 200 m per day, with 99% probability.
4. Maneuver Recovery - The velocity error in each component of the definitive orbit determination solutions 10 minutes after any maneuver shall not exceed either 1% of the associated components of the equivalent impulsive velocity vector or 25 mm/s, whichever is greater, with 99% probability.

The goal of this study is to determine if the navigation requirements can be met after incorporating post Preliminary Design Review** (PDR) changes in models and assumptions into the navigation simulations. These changes include updates to the simulation models to reflect the current MMS antenna design and the GPS acquisition characteristics observed using the Technology Readiness Level (TRL) 6 configuration of the Navigator receivers. Also considered is the sensitivity of the navigation performance to the onboard clock stability.

This paper is organized in three sections. The first section is the Simulation Approach which provides an overview of the simulation methodology and describes the orbital characteristics, trajectory generation parameters, data generation method, and filter settings that were used as well as a description of the cases run in this simulation. The second section presents the results and discusses how each of the above mentioned navigation requirements was verified and if each requirement was met. The final section summarizes conclusions and identifies areas of future work.

[§] Note that the minimum mean Phase 2b separation in the ROI has recently been raised from 25 km to 30 km.

** May 4 – 7, 2009

SIMULATION APPROACH

This section provides an overview of the simulation methodology used in this study and provides details regarding the orbital characteristics, trajectory generation, data generation, and filter settings. This section also discusses the five cases that were analyzed in this study.

Simulation Methodology

Figure 2 shows the simulation timeline used in this study. The timeline consists of an initial period of convergence followed by two formation maintenance maneuvers, a 9-day maneuver recovery period and a 7-day prediction period. In this simulation, the four satellites are maneuvered at the same time consistent with true anomalies of 202 and 158 degrees for satellite 1. Note that this will not be the case in actual operations because each spacecraft must be in contact with a ground station during the entire maneuver sequence and the spacecraft will not be simultaneously tracked. A realistic maneuver maintenance sequence covers about 1.5 hrs for all three spacecraft including 5 min Health and Safety (H&S) check, 5 min stored command load and verify, 5 min maneuver execution, 5 min propulsion safing verification, 5 min H&S check, 10 min handover between tracking contacts.

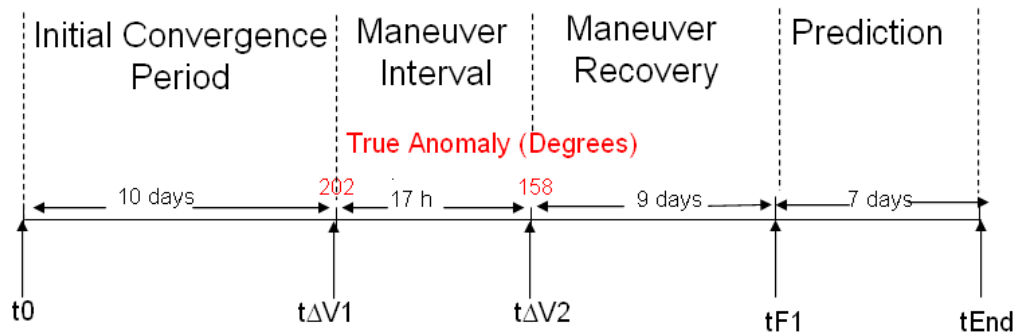


Figure 2: Formation Maintenance Simulation Timeline

An iterative simulation procedure (shown in Figure 3) was used so that the estimated state errors are included in the maneuver planning process. In each iteration, a truth trajectory is computed and used to simulate GPS pseudorange (PR) measurements, which are then processed in the GEONS filter. The formation maintenance maneuvers were modeled as impulsive maneuvers, which were computed using the Lambert Targeting algorithm in GEONS. This process is described in detail in Reference 1.¹ To ensure that the maneuvers have realistic magnitudes, the timeline started about 10 days before the next formation maintenance maneuvers using an initial truth state with errors consistent with steady-state filter performance and maneuver execution errors. The following times are used in the simulation:

- t0= simulation start time
- t Δ V1= time of formation maintenance maneuver 1
- t Δ V2= time of formation maintenance maneuver 2
- tF1= end time of filter processing
- tEnd= end time of prediction, tF1+7days

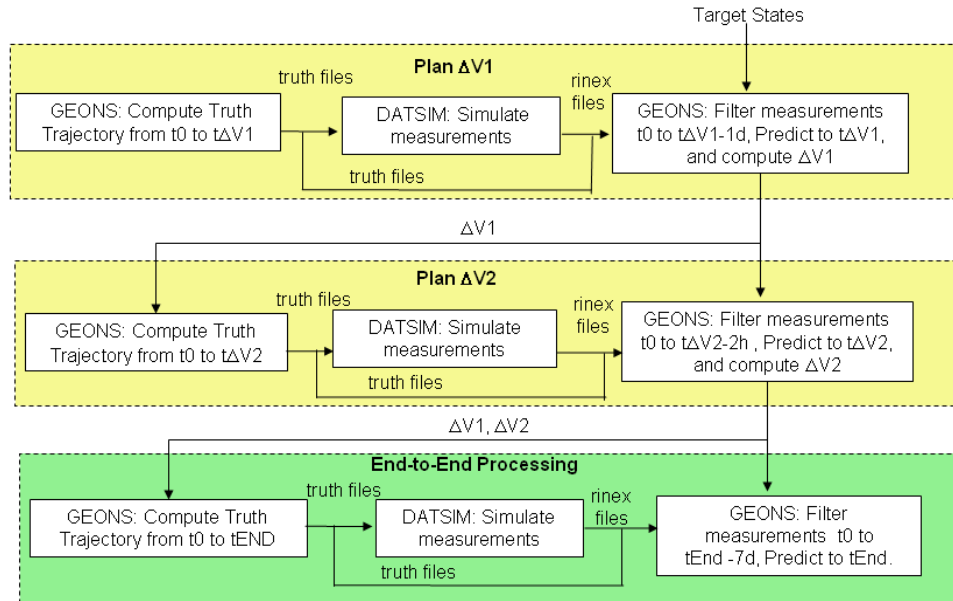


Figure 3: MMS Simulation Flow

The current study focuses on only the end-to-end processing portion of the simulation flow (bottom block in Figure 3). Maneuvers were computed for the PDR baseline configuration using the iterative procedure (top two blocks in Figure 3). The simulation steps are defined below:

1. Propagate truth trajectory from t_0 to $t_{\Delta V_2+16}$ days, applying ΔV_1 and ΔV_2 with the maneuver execution errors listed in Table 1.
2. Simulate GPS PR measurement data from t_0 to $t_{\Delta V_2+16}$ days using truth trajectory from step 4a.
3. Run GEONS to
 - i. Process measurement data t_0 to $t_{\Delta V_2+9}$ days (sufficient to achieve steady-state convergence), applying ΔV_1 and ΔV_2 with the maneuver knowledge errors listed in Table 2 and using a maneuver covariance consistent with the error in the maneuver model.
 - ii. Propagate the final estimated state for an additional 7 days.

Table 1: Maneuver Execution Errors

| | $\Delta V.X(mm/s)$ | $\Delta V.Y(mm/s)$ | $\Delta V.Z(mm/s)$ |
|-------|--------------------|--------------------|--------------------|
| MMS 1 | +6 | +6 | +6 |
| MMS 2 | -6 | -6 | -6 |
| MMS 3 | +6 | -6 | +6 |
| MMS 4 | -6 | +6 | -6 |

Table 2: Maneuver Knowledge Errors

| | $\Delta V.X(mm/s)$ | $\Delta V.Y(mm/s)$ | $\Delta V.Z(mm/s)$ |
|-------|--------------------|--------------------|--------------------|
| MMS 1 | +3 | +3 | +3 |
| MMS 2 | -3 | -3 | -3 |
| MMS 3 | +3 | -3 | +3 |
| MMS 4 | -3 | +3 | -3 |

Orbital Characteristics and Trajectory Generation

This section provides additional details for simulation step 1 including the models used and errors incorporated in generating the truth trajectory using GEONS. The initial truth reference formation orbital states for the satellites in this study are associated with a Phase 2b formation with a mean 25km separation in the ROI that satisfies the science quality factor requirements. The truth trajectories for this formation were generated using GEONS with the truth force model listed in Table 3. Figure 4 shows the associated relative separations based on the initial formation states. The minimum separation is approximately 8 km.

Table 3: Truth Trajectory Propagation Models

| Simulation Parameter | Nominal Values |
|----------------------------------|--|
| Nonspherical Earth Gravity Model | 30x30 JGM2 |
| Point Mass Gravity | Sun, Moon using DE 406 analytic ephemeris |
| Atmospheric Drag | Harris Priester model with solar flux=125 and C_D listed in Table 4. |
| Solar Radiation Pressure | Spherical model with C_R listed in Table 4 |
| Spacecraft Area | 3.3 meters ² |
| Spacecraft Mass | 865 kg (at beginning Phase 2b) |
| Integrator | 4 th order Runge-Kutta |
| Integration Stepsize | 10 seconds |
| Impulsive ΔV s | Planned values + maneuver execution errors found in Table 1 |

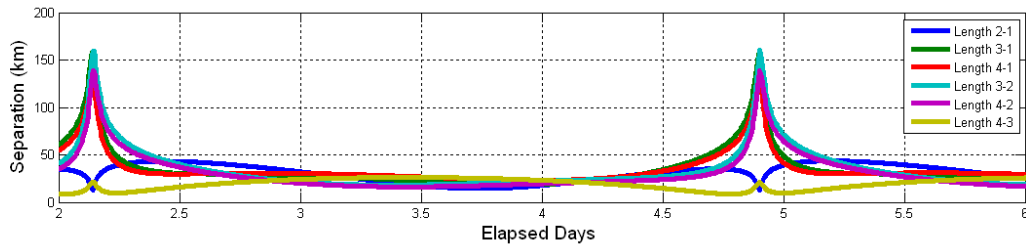


Figure 4: Initial Relative Separations

The area and mass of the spacecraft reflect values presented at the MMS Mission Design Review^{††}. It was assumed that common residual errors in the solar radiation pressure coefficient (C_R) are about 5%=0.07. For the uncorrelated relative C_R errors, it was assumed that spacecraft attitudes are maintained within 2 to 5 degrees of ecliptic normal and 30 degrees out of the plane formed by the normal to the ecliptic and the satellite-Sun vector. This difference corresponds to a 3-sigma relative C_R error of about 8%. These simulations used a relative C_R error of 5.6%. Similar assumptions were made for the atmospheric drag coefficient (C_D) errors. The coefficient values for the baseline simulation are as listed in Table 4.

Table 4: C_R and C_D Values Used in Truth Propagation

| MMS Satellite | 1 | 2 | 3 | 4 |
|---------------|------|------|------|------|
| C_D | 2.42 | 2.45 | 2.48 | 2.36 |
| C_R | 1.47 | 1.51 | 1.55 | 1.39 |

^{††} September 17-20, 2007

GPS Measurement Simulation

Simulation step 2 consists of simulating the GPS measurement data based on the truth trajectory. This section provides a description of the cases analyzed in this study, describes the measurement models used for each case, and discusses characteristics of the measurements simulated in this step.

Five cases were investigated in this study. The first case is the baseline for the MMS PDR. This simulation is discussed in detail in Reference 1.¹ The antenna model in Case 1 has antennas mounted on the top and bottom of a non-spinning spacecraft. Case 2 differs from Case 1 in that it (1) uses a reduced measurement rate of every 30 seconds, (2) has a larger clock scale factor of 1, (3) incorporates a new antenna model that models the current design of four antennas located with boresights in the plane normal to the spin axis, and (4) has a higher signal acquisition threshold. Case 3 differs from Case 2 in that (1) GPS ephemeris errors were added, (2) the measurements are simulated every 10 seconds in order to simulate realistic GPS ephemeris errors using a correlated ephemeris error model available in the Measurement Data Simulation Program (DATSIM) but measurements are processed only every 30 seconds, and (3) GPS SV selection criteria were varied for each spacecraft. Cases 4 and 5 are identical to Case 3 except the clock scale factor is increased by a factor of 7 for Case 4 and a factor of 30 for Case 5. Larger clock scale factors yield less stable clock behavior. The differences between the cases are further described in Table 5 through Table 7 as well as Table 9 in the section below.

Table 5 through Table 7 summarize the measurement data simulation parameters. The measurement noise levels are based on Navigator TRL5 levels, which are consistent with initial TRL6 test results. The GPS acquisition probability is based on initial TRL6 tests. Note that these tables are divided up to indicate the differences between the cases. Figure 5 compares the number of GPS space vehicles (SVs) that can be acquired based on 25 dB-Hz versus 28 dB-Hz acquisition thresholds with the acquisition probabilities listed in Table 6 and limiting the GPS tracking to below the science ROI, which is $< 15R_E$ for Phase 2b. The time period in each orbit when GPS signals cannot be acquired is about 50 hours out of the 2.8 day orbit. There is a 27% reduction in the number of GPS measurements in Case 3 versus Case 1. Variations in the GPS SVs selection criteria in Cases 3 through 5 resulted in a maximum of 4 out of 12 GPS SVs being different among the satellites, out of the maximum of 16 that could be acquired at perigee.

Table 5: Navigation Error Models for All Cases

| Simulation Parameter | Nominal Values for All Cases |
|--|---|
| 1-sigma GPS Pseudorange Noise | 4.4 meters above 38 dB-Hz 6.1 meters for (30-38) dB-Hz 8.8 meters for (25-30) dB-Hz |
| Ionospheric Delay Model | GPS Ionospheric Model based on GPS broadcast ionospheric coefficients |
| Minimum Height of Ray Path Altitude | 1000 km (eliminates measurements with largest ionospheric delays) |

Table 6: GPS Measurement Simulation Models

| Simulation Parameter | Nominal Values for Cases 1 and 2 | Nominal Values for Cases 3, 4, and 5 |
|---|--|--|
| GPS Pseudorange Measurement Rate | 1 Measurement set every 10 seconds for Case 1 and 30 seconds for Case 2 for each formation member with measurements from a maximum of 12 visible GPS SVs | 1 Measurement set every 10 seconds with observations processed every 30 seconds for each formation member with measurements from a maximum of 12 visible GPS SVs |
| GPS Ephemeris Error Sigma | 0.0 m | 2.0 m |
| GPS SV Selection | | |
| MMS1 | Antenna gain, max to min values | Antenna gain, max to min values |
| MMS2 | Antenna gain, max to min values | Antenna gain, min to max values |
| MMS3 | Antenna gain, max to min values | Transmitter ID, max to min values |
| MMS4 | Antenna gain, max to min values | Transmitter ID, min to max values |

Table 7: Navigator Receiving Antenna Model

| Simulation Parameter | Case 1 | Cases 2 through 5 |
|--|---|--|
| Navigator Receiving Antenna Model | Peak gain in the North and South directions with respect to the ecliptic plane | Composite toroidal model with peak gain in the plane normal to the spin axis |
| GPS Acquisition Threshold | >45dB-Hz with 100% probability of acquisition with a minimum acquisition delay of 600 sec 41 to 45 dB-Hz with 95% probability of acquisition with a minimum acquisition delay of 600 sec 25 to 41 dB-Hz with 75% probability of acquisition with a minimum acquisition delay of 600 sec Data in the ROI removed. | 41 to 60 dB-Hz with 95% probability of acquisition with a minimum acquisition delay of 600 sec 28 to 41 dB-Hz with 75% probability of acquisition with a minimum acquisition delay of 600 sec Data in the ROI removed. |
| GPS Antenna Model | GPS IIA attenuation table with +3dB gain above specs | GPS IIA attenuation table with minimum gain |

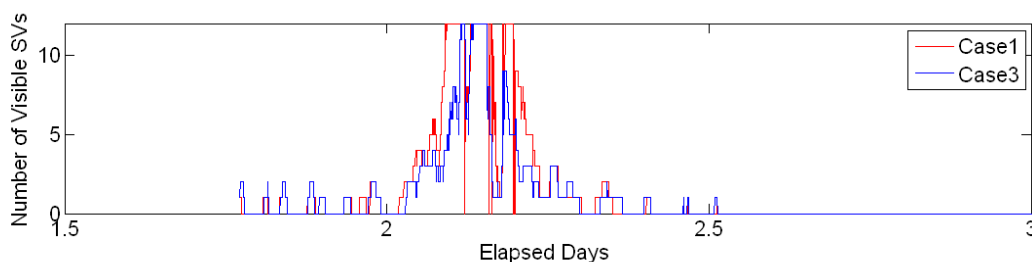


Figure 5: GPS Visibility for 1 Perigee Passage for MMS4 - Cases 1 and 3

Table 8 and Table 9 list the clock error parameters used to simulate the true clock bias for each satellite for each case. The h_0 and h_{-2} values in two of the columns below are the coefficients of the phase noise power spectral density curve, which are related to the Allan Variance Parameters. Table 9 shows the variation in clock scale factor values for all the cases. The scale factor values for Case 1 were selected to simulate maintenance of the clock bias to within 25 microseconds. Larger scale factors produce less stable clock behavior.

Table 8: MMS Clock Error Models for All Cases

| Satellite | Clock Parameter | | | |
|-----------|-----------------|--------------|----------|---------|
| | Initial Bias | Initial Rate | h_0 | h_2 |
| MMS1 | -1.6343D-05 | 0 | 2.40D-22 | 8.0D-28 |
| MMS 2 | -1.7309D-05 | 0 | 2.40D-22 | 8.0D-28 |
| MMS 3 | 3.0237D-05 | 0 | 2.40D-22 | 8.0D-28 |
| MMS 4 | -2.9469D-05 | 0 | 2.40D-22 | 8.0D-28 |

Table 9: Clock Scale Factors for Each Case

| Satellite | Clock Scale Factor | | | | |
|-----------|--------------------|--------|--------|--------|--------|
| | Case 1 | Case 2 | Case 3 | Case 4 | Case 5 |
| MMS1 | 0.1 | 1 | 1 | 7 | 30 |
| MMS2 | 0.5 | 1 | 1 | 7 | 30 |
| MMS3 | 0.3 | 1 | 1 | 7 | 30 |
| MMS4 | 0.5 | 1 | 1 | 7 | 30 |

Filter Settings

Simulation step 3 consists of processing the simulated measurements in the GEONS filter to estimate the spacecraft states. The filter relied upon inputs from both the truth trajectory and the GPS measurements, both of which were described above. This section provides details for the filter process including the models used and the settings for the filter. Table 10 and Table 11 contain the nominal GEONS filter settings that were used in this study to estimate all spacecraft independently using filter parameters based on References 2 and 3.^{2,3}

Table 10: GEONS Filter Trajectory Propagation Models

| Parameter | Nominal Values |
|----------------------------------|---|
| Nonspherical Earth Gravity Model | 8x8 JGM2 |
| Point Mass Gravity | Sun, Moon using analytical fit to DE 406 ephemeris |
| Atmospheric Drag | Analytical fit to Harris Priester model with solar flux=125 and $C_D=2.2$ |
| Solar Radiation Pressure | Spherical model with $C_R=1.4$ |
| Spacecraft Area | 3.3 meters ² |
| Spacecraft Mass | 865 kg |
| Integrator | 4 th order Runge-Kutta |
| Integration Stepsize | 10 seconds |

Table 11: GEONS Filter Settings

| Parameter | Nominal Values |
|--|--|
| Estimation State | $\bar{r}, \dot{\bar{r}}, b_R, d_R$ for all 4 spacecraft |
| Estimation Option | Absolute state vector estimation |
| Initial position and velocity state errors | 300 m and 15 mm/sec per axis (3-sigma) |
| Initial Clock bias and drift errors | 7.5 km (25 microseconds) and .03 m/sec (0.0001 microseconds/sec) (1-sigma) |
| Initial Position and Velocity Covariance | 3e5 m ² and 3e-4 m ² /s ² per axis |
| Initial Clock Bias and Drift Covariance | 1e8 m ² and 2e-3 m ² /s ² per axis |
| RIC Velocity Process Noise Variance Rate | 1e-13, 1e-12, 1e-12 m ² /s ³ |
| Clock Bias and Drift Process Noise Variance Rate | 10e-5 m ² /s, 10e-5 m ² /s ³ |
| GPS PR standard deviation | 40 m |
| Maneuver Variances | 1E-5 m ² /s ² for M1 and 5E-5 m ² /s ² for M2 per axis starting about 1 hr prior to and ending about 1 hr following each maneuver time |

Summary of Maneuvers

Table 12 and Table 13 list the values for the first and second formation maintenance maneuvers, respectively. The values in Table 12 and Table 13 were obtained using the maneuver planning process discussed in the Simulation Methodology section. The errors applied to the formation maintenance maneuvers are listed in Table 1 and Table 2. The baseline formation maintenance maneuver concept is to maneuver three of the four spacecraft each time to achieve the correct relative separation with the non-maneuver spacecraft following the final maneuver. In this simulation, the target vector was computed in GMAT (Reference 4) ⁴ based on the propagated initial state vector rather than the propagated filter vector for satellite 1. For this reason a small maneuver was also needed for satellite 1 to achieve the target state. Note that the second maneuver is being retargeted simplistically because the method used corrects for the velocity error but not the position error.

Table 12: Maneuver 1

| | Time | | $\Delta V1.X(m/s)$ | $\Delta V1.Y(m/s)$ | $\Delta V1.Z(m/s)$ |
|-------|-------|-----------|--------------------|--------------------|--------------------|
| | Start | End | | | |
| Sat 1 | 57764 | 82490.773 | -2.92E-03 | -9.04E-03 | -3.51E-03 |
| Sat 2 | 57764 | 82490.773 | -5.66E-01 | -1.14E-01 | -1.67E-02 |
| Sat 3 | 57764 | 82490.773 | -3.78E-01 | -2.15E-01 | -8.90E-02 |
| Sat 4 | 57764 | 82490.773 | -4.31E-01 | -1.75E-01 | -1.24E-01 |

Table 13: Maneuver 2

| | Time | | $\Delta V2.X(m/s)$ | $\Delta V2.Y(m/s)$ | $\Delta V2.Z(m/s)$ |
|-------|-------|-----------|--------------------|--------------------|--------------------|
| | Start | End | | | |
| Sat 1 | 57765 | 57213.475 | -3.91E-03 | -4.17E-03 | 2.75E-03 |
| Sat 2 | 57765 | 57213.475 | -4.43E-01 | 3.92E-01 | 1.55E-01 |
| Sat 3 | 57765 | 57213.475 | -2.84E-01 | 6.67E-02 | 2.30E-02 |
| Sat 4 | 57765 | 57213.475 | -3.31E-01 | 1.70E-01 | 6.00E-02 |

SIMULATION RESULTS

The following subsections address the four navigation requirements investigated in this study. Each subsection describes how the requirement was verified and if the requirement is met for the cases analyzed in this study. A detailed description of these requirements is provided in the Introduction section. Table 14 contains a summary of the cases examined in this study.

Table 14: Summary of Cases

| Case | Antenna Peak Gain Direction | Measurement Rate (seconds) | Measurement Processing Frequency | SV Selection Order | Clock Scale Factor |
|------|--|----------------------------|----------------------------------|--------------------|--------------------|
| 1 | North/South with respect to ecliptic plane | 10 | 1 | Constant | 0.1-0.5 |
| 2 | Plane normal to spin axis | 30 | 1 | Constant | 1 |
| 3 | Plane normal to spin axis | 10 | 3 | Varied | 1 |
| 4 | Plane normal to spin axis | 10 | 3 | Varied | 7 |
| 5 | Plane normal to spin axis | 10 | 3 | Varied | 30 |

Definitive Absolute Orbit Determination

Figure 6 contains the maximum root-sum-square (RSS) position error for each case during the definitive period following initial filter convergence (i.e., days 3 through 20). The value shown for each case is the maximum of the four MMS spacecraft. The maximum definitive position error requirement of 100 km is met in all cases. The antenna changes seen in going from Case 1 to Case 2 along with the clock scale factor changes seen in going from Case 3 to Cases 4 and 5 had negative impacts on the maximum absolute definitive position errors, which occur during the orbit immediately following the formation maintenance maneuvers. In all cases, maximum error, which occurs in the ROI immediately following maneuver 2, is much smaller than the root variance error in that region of 98km.

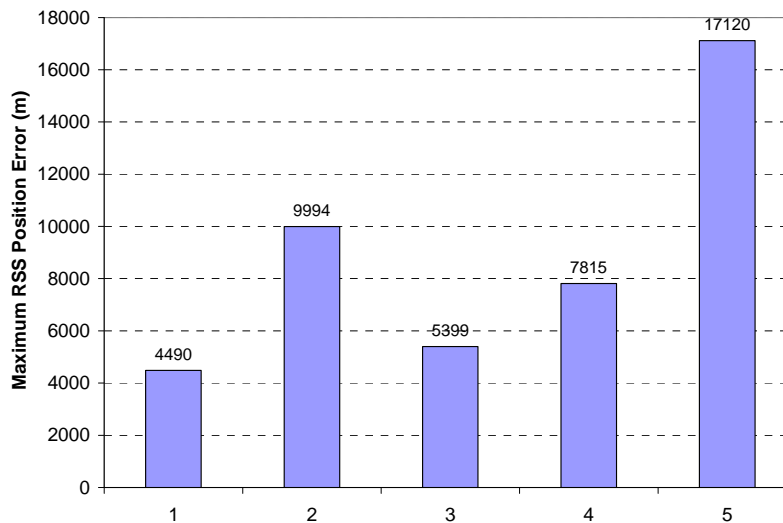


Figure 6: Maximum Definitive Absolute RSS Position Error

The steady-state behavior is very similar in all cases. The figures below show the absolute RSS position errors for each case as black solid lines and the root-variance values as red dashed lines. The position errors are shown for the MMS satellite with the largest maximum values. Note that in these figures the y-axes have different scales. The maximum absolute position errors over 7 day predictions remain below 2000m in all cases.

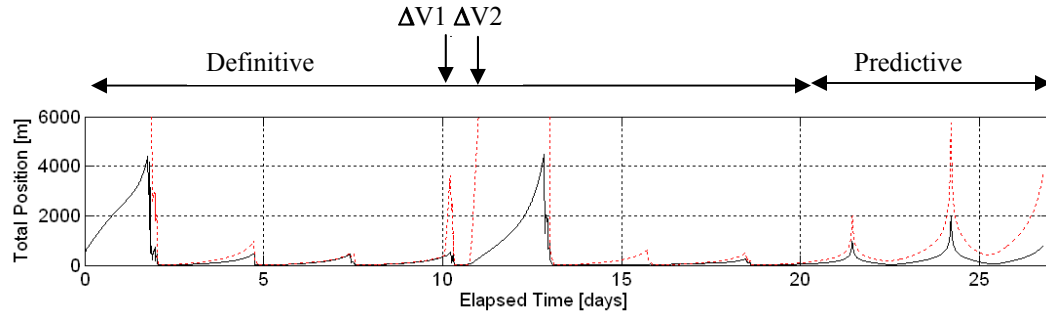


Figure 7: Absolute RSS Position Error for MMS1 Showing Maximum for Case 1

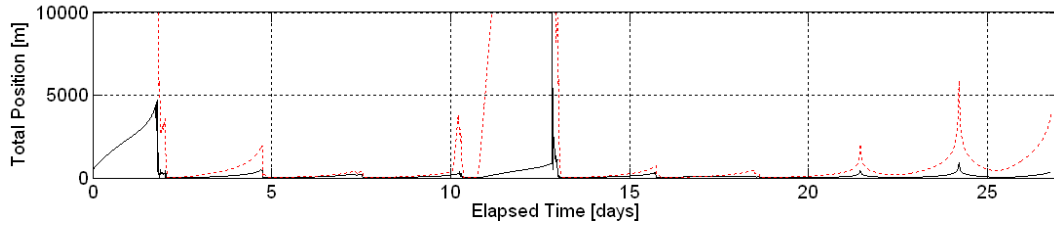


Figure 8: Absolute RSS Position Error for MMS4 Showing Maximum for Case 2

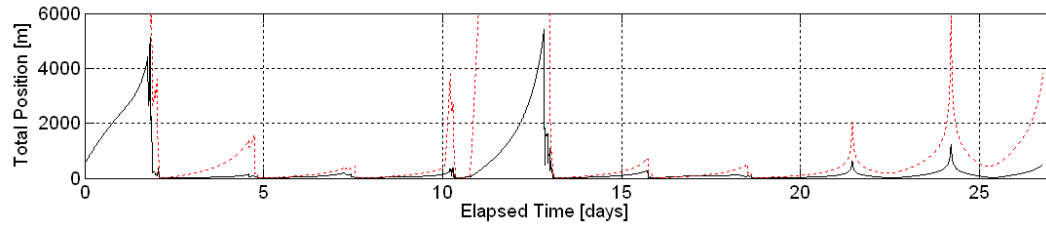


Figure 9: Absolute RSS Position Error for MMS1 Showing Maximum for Case 3

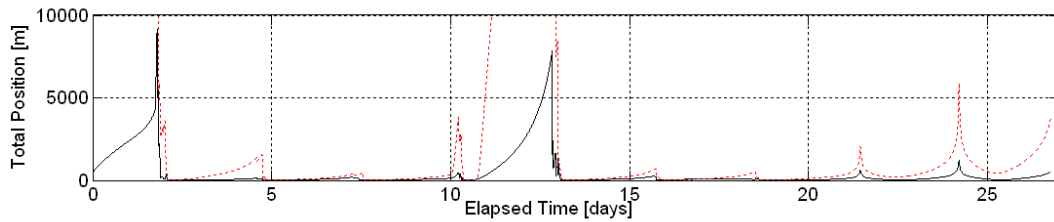


Figure 10: Absolute RSS Position Error for MMS1 Showing Maximum for Case 4

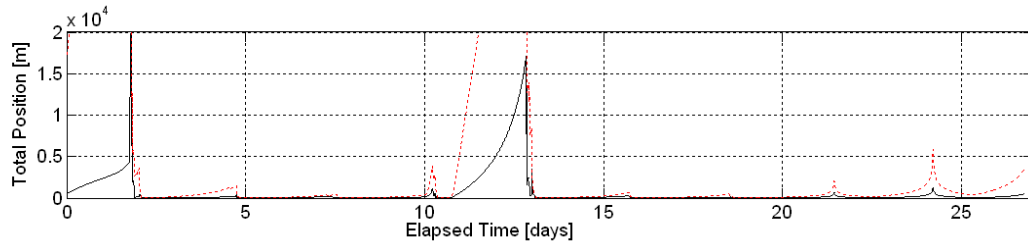


Figure 11: Absolute RSS Position Error for MMS1 Showing Maximum for Case 5

Definitive Relative Orbit Determination

Figure 12 contains the maximum relative definitive RSS position errors during all the ROIs following initial filter convergence except for the ROI immediately following the maneuvers. The changes in the antenna model had a slight impact on the errors. Variations in the selection of the GPS SVs had the largest impact. Figure 13 contains the maximum relative definitive RSS position errors during all the ROIs following initial filter convergence including the ROI immediately following the maneuvers. These values are significantly larger than those seen in Figure 12. In Figure 13, increasing the clock scale factor makes a significant impact on the position error increase. The new antenna model makes a slight impact as well.

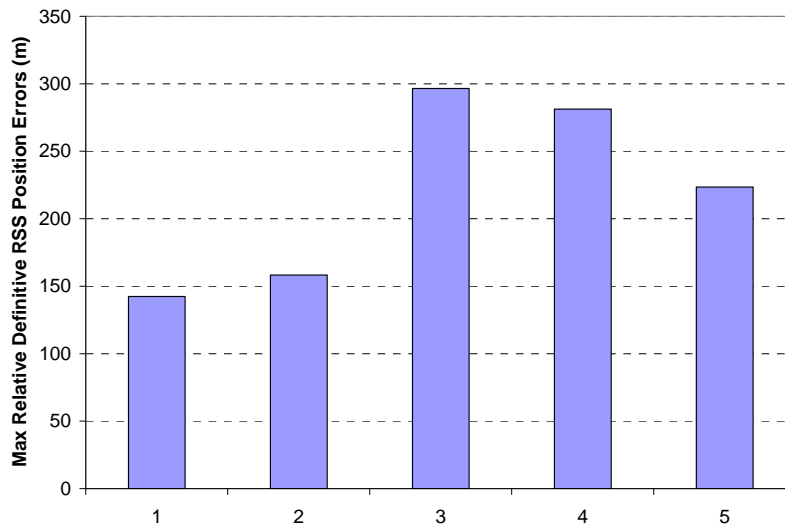


Figure 12: Maximum Relative Definitive RSS Position Errors in ROI Not Including Post-Maneuver ROI

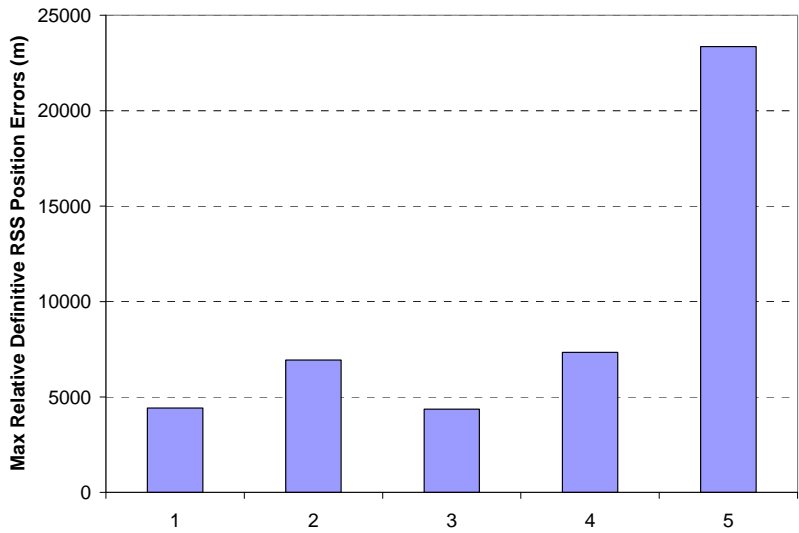


Figure 13: Maximum Relative Definitive RSS Position Errors in ROI Including Post-Maneuver ROI

The plots in Figure 14 show the relative orbit determination errors compared with the requirement and verify that this requirement is met except during the ROI immediately following the formation maintenance maneuvers for Case 3. Case 3 is shown because it is the case that most resembles the current design. Note that the requirement applies in the ROI immediately following formation maintenance maneuvers and is not met by any case in this analysis. If the requirement cannot be satisfied onboard, processing will have to be performed on the ground after the fact. In these figures, the blue solid lines are the errors, the green solid lines are the requirements during ROI, and the red dotted lines are the RSS estimated root-variance values. The estimated root-variance values are large because of the correlations between unmodeled dynamic errors such as those that arise from truncation of the gravity model and solar radiation pressure cross-sectional area errors.

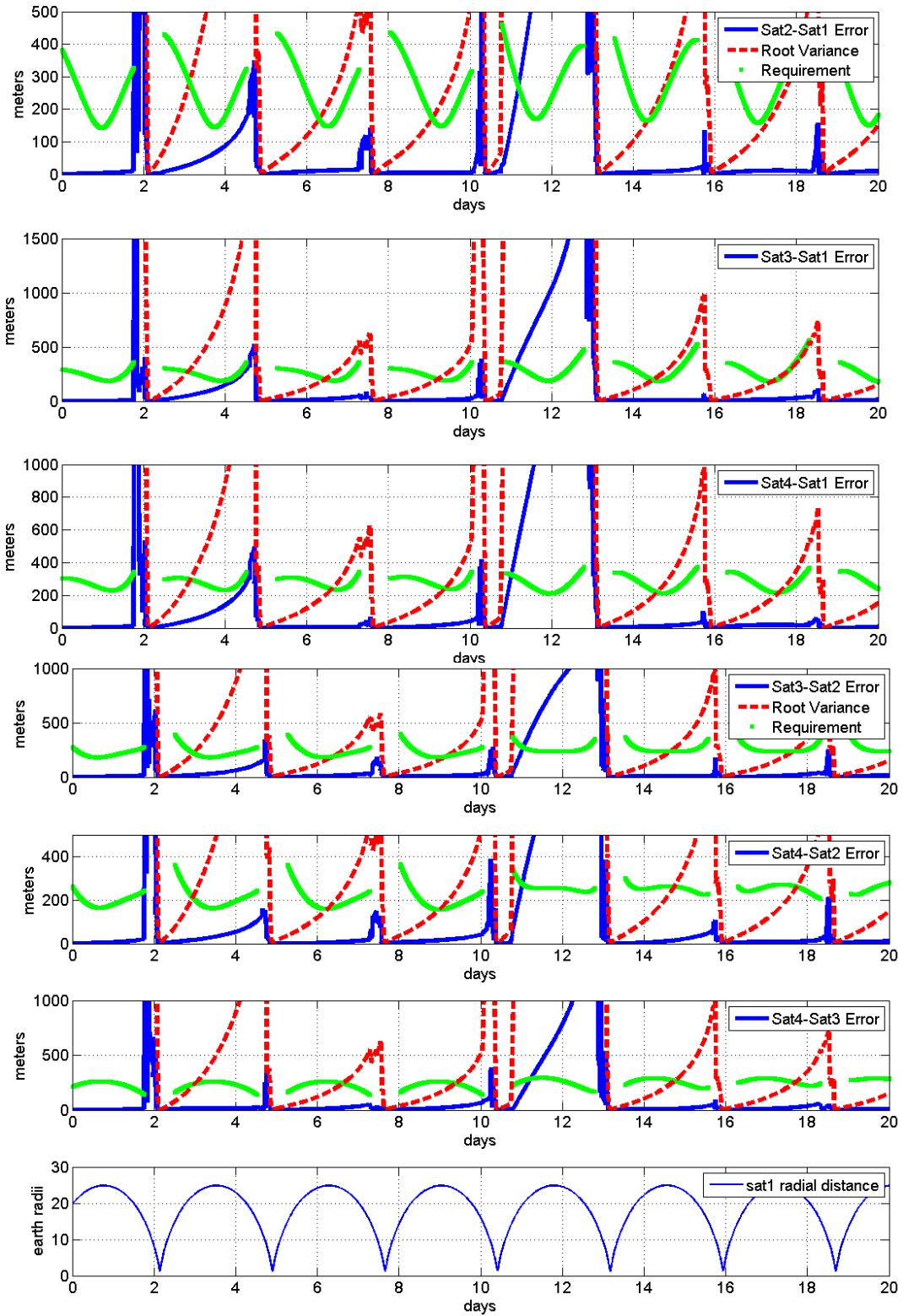


Figure 14: Relative Definitive Position Errors for Case 3

Predictive Relative Orbit Determination

Figure 15 compares the relative predictive position error growth rate mean and maximum for the four satellites for each of the cases. Table 15 contains the relative predictive position error growth rate for each spacecraft for each case. The requirement is never violated for any of the cases. The relative error growth rate is most sensitive to the change in the antenna models used in Cases 2 through 5. The GPS SV variation in Case 3 or larger clock scale factors in Cases 4 and 5 do not have a large impact on the relative prediction position error growth rate or any of the other requirements being met. The plots in Figure 16 contain the relative prediction position errors for Case 3, which is the case closest to the current navigation design.

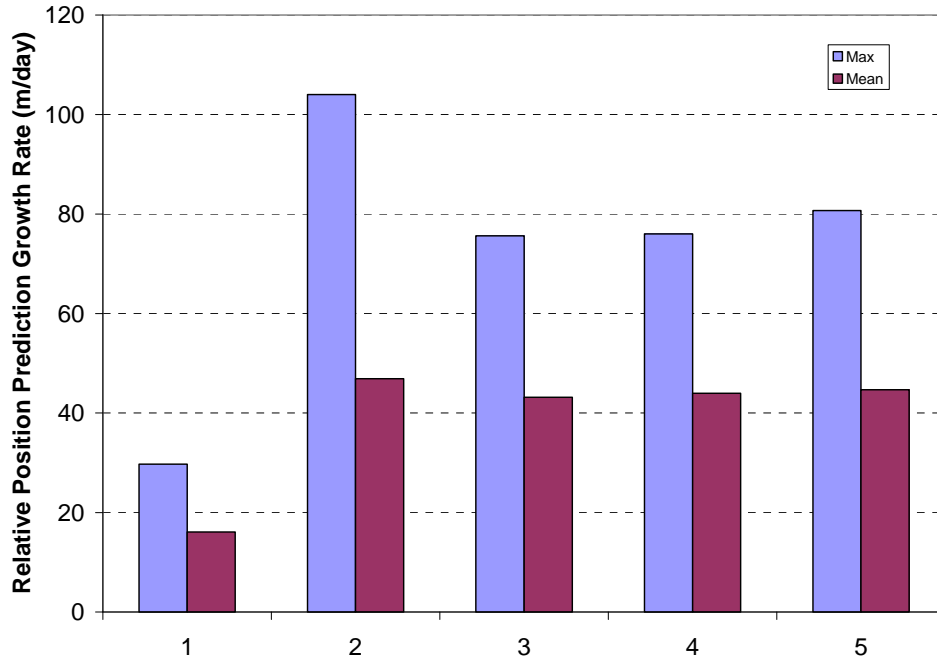


Figure 15: Relative Predictive RSS Position Growth Rate

Table 15: Relative Predictive RSS Position Growth Rate (m/day)

| Case | MMS2-1 | MMS3-1 | MMS4-1 | MMS3-2 | MMS4-2 | MMS4-3 |
|------|--------|--------|--------|--------|--------|--------|
| 1 | 5 | 3 | 30 | 5 | 25 | 28 |
| 2 | 45 | 4 | 41 | 49 | 104 | 39 |
| 3 | 28 | 76 | 61 | 48 | 34 | 13 |
| 4 | 27 | 76 | 59 | 49 | 32 | 21 |
| 5 | 26 | 81 | 51 | 55 | 25 | 30 |

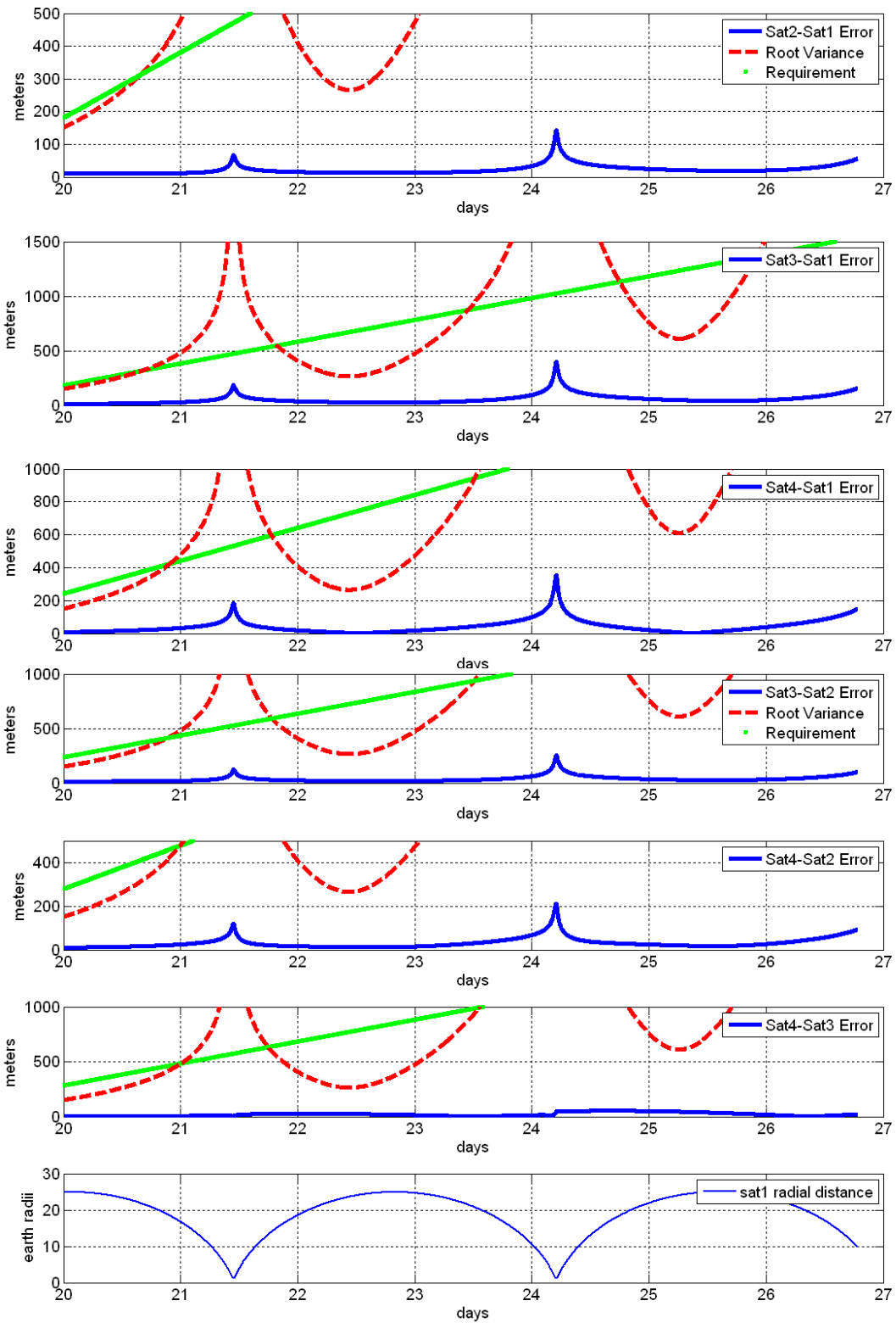


Figure 16: Relative Predictive Position Errors for Case 3

Maneuver Recovery

The maneuver recovery requirement is 25 mm/s for this simulation because 25 mm/s is greater than 1% of the associated components of the equivalent impulsive velocity vector listed in Tables 12 and 13. Figure 17 and Figure 18 indicate the maneuver recovery requirement of 25 mm/s after 10 minutes is met in all the cases although it is close to the limit for maneuver 2 in Case 5. The numbers shown in these two figures are the maximum component values from the four spacecraft for each case. The clock scale factor makes a significant impact on the velocity error immediately following a maneuver.

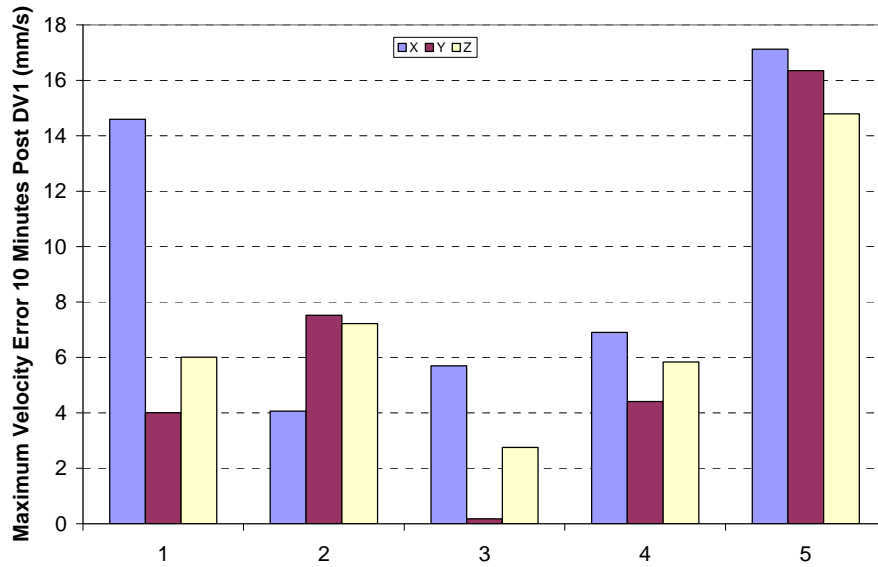


Figure 17: Maximum RSS Velocity Error 10 Minutes Post DV 1

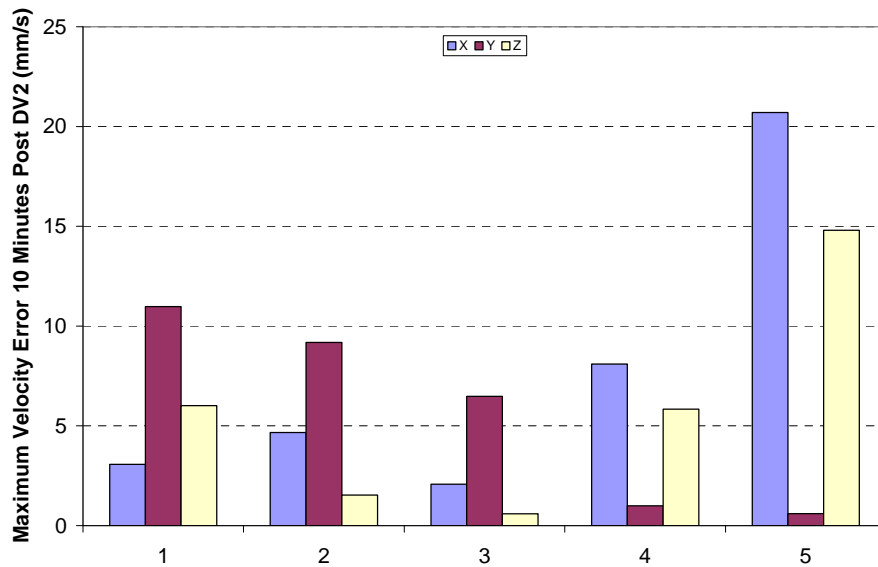


Figure 18: Maximum Velocity Error 10 Minutes Post DV 2

The following figures show that approximately 10 minutes after each maneuver, the RSS velocity error is less than 25 mm/s for Cases 1 through 4. Note that in Figure 19 through Figure 23, the black solid line is the error and the red dashed line is the root-variance.

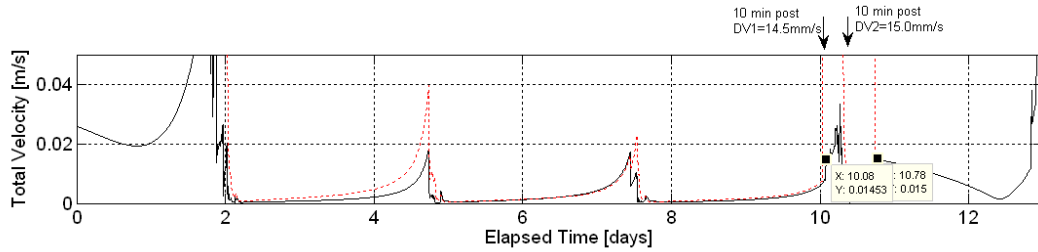


Figure 19: Absolute Definitive Velocity Error for MMS3 for Case 1

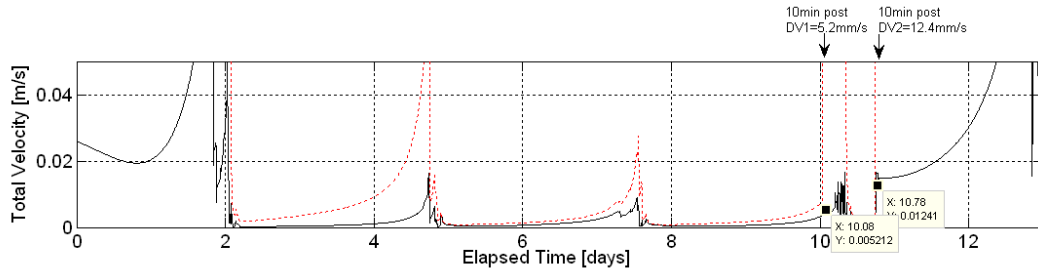


Figure 20: Absolute Definitive Velocity Error for MMS2 for Case 2

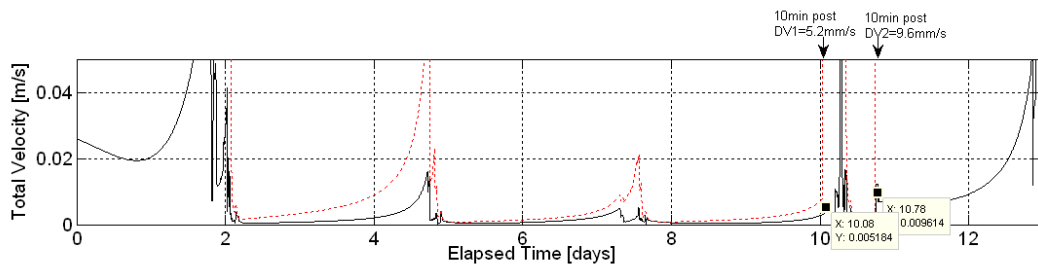


Figure 21: Absolute Definitive Velocity Error for MMS2 for Case 3

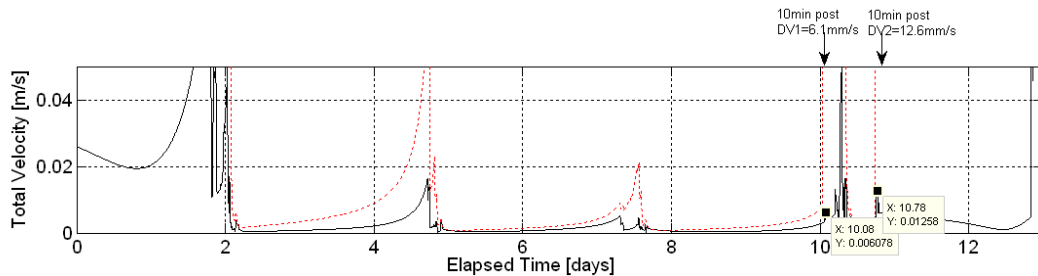


Figure 22: Absolute Definitive Velocity Error for MMS2 for Case 4

Figure 23 shows the definitive velocity error for MMS2 for Case 5, which has the largest error at 10 minutes after maneuver 2. Figure 23 shows that approximately 10 minutes after the second maneuver, the RSS error is greater than 25 mm/s; however, each component's error is less than 25 mm/sec.

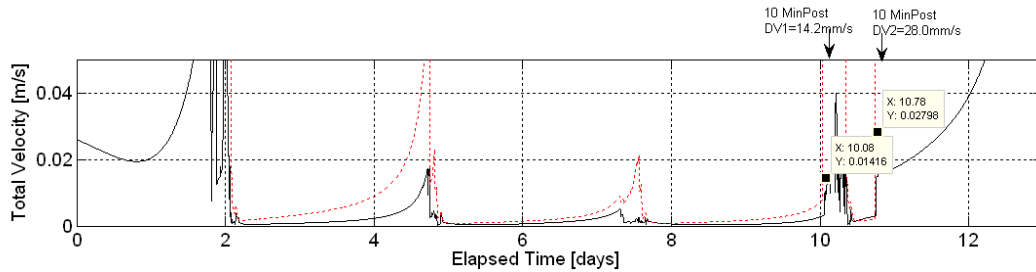


Figure 23: Absolute Definitive Velocity Error for MMS2 for Case 5

CONCLUSIONS AND FUTURE WORK

Navigation performance during Phase 2b of the MMS mission was evaluated with respect to the navigation requirements for definitive absolute orbit determination, definitive relative orbit determination, predictive relative orbit determination, and maneuver recovery. This analysis shows that for each Phase 2b, 25km separation case evaluated, the navigation requirements are met except for the relative definitive position error requirement in the ROI immediately following the formation maintenance maneuver. In addition, the maneuver recovery requirement is close to being violated when the receiver's clock is significantly less stable than its specifications, because clock stability has a significant impact on the ability of the navigation solution to quickly reconverge following each formation maintenance maneuver. The relative definitive position error requirement immediately following the formation maintenance maneuver is violated in every case examined in this study, indicating that ground post-processing will probably be required to meet this requirement.

Future studies are planned in which acceleration files will be included for the small maneuvers being performed in Phase 2b. Extensive Monte Carlo simulations are planned to verify that the 99% probability requirement can be met. These simulations will include updated Navigator TRL6 acquisition probabilities, reacquisition times, and noise performance values based on completion of TRL6 tests as well as using reference trajectories for nominal launch window. These simulations will also include acceleration measurement errors and maneuver execution errors. In addition, ground post-processing procedures will be developed to improve navigation performance during maneuver recovery periods.

REFERENCES

- ¹ Paige Thomas Scaperoth and Anne Long, "MMS Phase 2b, 25km Separation Formation Maintenance Navigation Analysis," MMS-FD-2009-101, March 5, 2009.
- ² Paige Thomas Scaperoth and Anne Long, "MMS Phase 2b Formation Maintenance Scenario with 1-Way DSN Doppler Tracking," MMS-FD-2008-125, July 28, 2008.
- ³ Taesul Lee and Michael Volle, "Magnetospheric Multiscale (MMS) Mission Maneuver Recovery Analysis," FDF-59-013, February 8, 2007.
- ⁴ General Mission Analysis Tool (GMAT). <http://gmat.wiki.sourceforge.net/>